



# A genetic meta-algorithm-assisted inversion approach: hydrogeological study for the determination of volumetric rock properties and matrix and fluid parameters in unsaturated formations

Norbert Péter Szabó<sup>1,2</sup>

Received: 6 May 2017 / Accepted: 16 February 2018  
 © Springer-Verlag GmbH Germany, part of Springer Nature 2018

## Abstract

An evolutionary inversion approach is suggested for the interpretation of nuclear and resistivity logs measured by direct-push tools in shallow unsaturated sediments. The efficiency of formation evaluation is improved by estimating simultaneously (1) the petrophysical properties that vary rapidly along a drill hole with depth and (2) the zone parameters that can be treated as constant, in one inversion procedure. In the workflow, the fractional volumes of water, air, matrix and clay are estimated in adjacent depths by linearized inversion, whereas the clay and matrix properties are updated using a float-encoded genetic meta-algorithm. The proposed inversion method provides an objective estimate of the zone parameters that appear in the tool response equations applied to solve the forward problem, which can significantly increase the reliability of the petrophysical model as opposed to setting these parameters arbitrarily. The global optimization meta-algorithm not only assures the best fit between the measured and calculated data but also gives a reliable solution, practically independent of the initial model, as laboratory data are unnecessary in the inversion procedure. The feasibility test uses engineering geophysical sounding logs observed in an unsaturated loessy-sandy formation in Hungary. The multi-borehole extension of the inversion technique is developed to determine the petrophysical properties and their estimation errors along a profile of drill holes. The genetic meta-algorithmic inversion method is recommended for hydrogeophysical logging applications of various kinds to automatically extract the volumetric ratios of rock and fluid constituents as well as the most important zone parameters in a reliable inversion procedure.

**Keywords** Geophysical methods · Genetic algorithm · Zone parameter · Unsaturated zone · Hungary

## Introduction

Direct-push measurements are widely used for the in-situ characterization of shallow water-bearing formations. Geophysical logging tools are usually incorporated in the cone-penetration equipment for a more detailed and reliable site investigation. Nuclear measurements are normally applied to estimate the shale volume, porosity and

water saturation in unconsolidated formations. The electrical conductivity log is applicable for a general hydrostratigraphic analysis by giving information on the vertical variations in hydraulic conductivity (Butler 2005). By using the surface geoelectric method using special electrode arrays, the drillhole information can be spatially extended and the results of hydrogeophysical interpretation can be effectively improved (Szalai et al. 2015). Detailed facies mapping can also be done by the lateral correlation of electric logs measured in neighboring drill holes (Schulmeister et al. 2003). Recently an inexpensive nuclear magnetic resonance probe was developed to separate the mobile and bound water fractions and provide information on the pore-size distribution and hydraulic conductivity in direct-push drill holes (Walsh et al. 2013). Additional data acquisition techniques such as

✉ Norbert Péter Szabó  
 norbert.szabo.phd@gmail.com

<sup>1</sup> Department of Geophysics, University of Miskolc, Miskolc-Egyetemváros 3515, Hungary

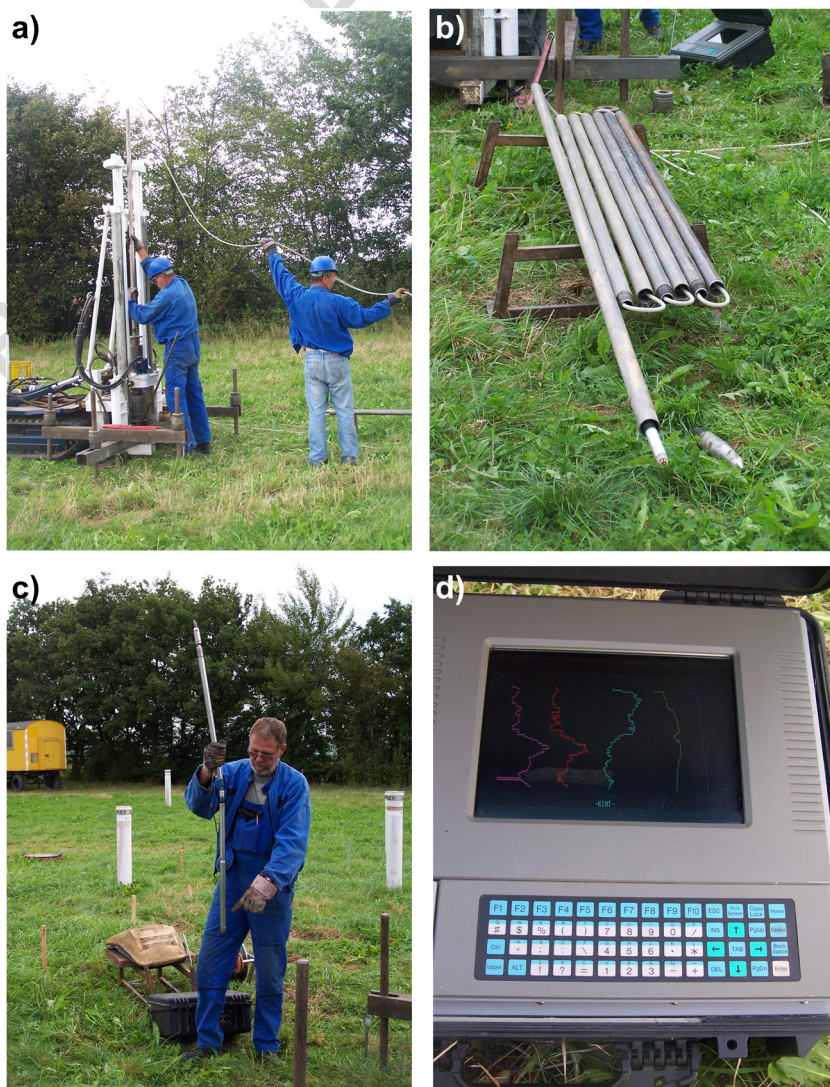
<sup>2</sup> Geoengineering Research Group, [MTA-ME, Miskolc-Egyetemváros 3515, Hungary

54 hydrogeochemical, seismic and tomographic measure- 72  
 55 ments, and groundwater and soil gas sampling possibili- 73  
 56 ties, are detailed in Kirsch (2006). 74

57 A direct-push technology called engineering geophysical 75  
 58 sounding (EGS) was developed to solve environmental and 76  
 59 groundwater problems in Hungary (Fejes and J6sa 1990). In 77  
 60 addition to conventional geotechnical parameters such as cone 78  
 61 resistance and sleeve friction, the EGS instruments observe 79  
 62 the natural gamma radioactivity, neutron-porosity, bulk den- 80  
 63 sity and electrical resistivity in a drill hole. During the measure- 81  
 64 ment, a steel tube is pushed into the ground (Fig. 1a), which is 82  
 65 the only material that separates the sensor from the soil. The 83  
 66 observed data are transferred to the surface unit through the 84  
 67 rods (Fig. 1b). Since there is no invasion of drilling fluid into 85  
 68 the formation, the measured data should not be corrected for 86  
 69 borehole effects. The EGS data collected by different probes 87  
 70 (Fig. 1c) are recorded in digital format and represented by drill 88  
 71 hole logs (Fig. 1d).

The geophysical model used in this study for describing the 72  
 petrophysical characteristics of the unsaturated zone contains 73  
 two types of parameters. In addition to the fractional volumes 74  
 of rock constituents and pore-filling fluids, one has to deter- 75  
 mine a certain number of zone parameters including the phys- 76  
 ical properties of clay, fluids and minerals, and the textural 77  
 features of rocks. The parameters of the first group change 78  
 rapidly with the depth, while the zone parameters are almost 79  
 constant in the entire domain of the geophysical sounding (the 80  
 maximum penetration depth is 20–30 m in loose sediments). 81  
 The model parameters included in the probe response equa- 82  
 tions are normally estimated by solving a local inverse prob- 83  
 lem at a given depth. Since having a smaller number of data 84  
 types than unknowns at the depth point, the zone parameters 85  
 are normally treated as constant, the initial values of which 86  
 are a priori given using laboratory data or by literature. If 87  
 the zone parameters were estimated by local inversion, an 88  
 underdetermined inverse problem should be solved for an 89

**Fig. 1** Engineering geophysical sounding operation in J6lich, Germany: **a** the drill rod is being connected to the others that have been pushed into the ground, **b** wired rods prepared for measurement with a connector and a cone head, **c** combined gamma-ray probe used for the measurement of natural gamma-ray intensity and formation density, **d** real-time visual display of observed parameters on the screen of E1009-type surface unit



90 infinite number of solutions. In that case, the problem of  
91 ambiguity and numerical instability of the inversion  
92 procedure could not be avoided. Instead of this, Drahos  
93 (2005) suggested solving an overdetermined (local) in-  
94 verse problem to give an estimate to the volumetric rock  
95 properties by fixed zone parameters. In order to compen-  
96 sate for different measurement accuracies and scales, the  
97 weighted least squares method is applied (Menke 1984).  
98 The preceding EGS inversion approach is very quick, but  
99 rather noise sensitive, as there is barely more data than  
100 unknowns at a given depth. Moreover, it requires the  
101 choice of appropriate zone parameters, which may pose a  
102 risk, because the inversion procedure is exposed to uncon-  
103 trolled modeling error.

104 So far, there has not been significant progress in the  
105 automated determination of zone parameters even in  
Q1 106 oilfield-well-log analysis. Narayan and Yadav (2006) give  
107 a least squares estimate to a limited number of matrix  
108 parameters, where only the mean values of observed well  
109 logs are optimized in a particular water-bearing horizon.  
110 The zone parameters of quartz and water are fixed during  
111 the optimization procedure, while those of other minerals  
112 (if present) are changed to a maximum of 20% of their  
113 initial values originally given by cross-plot techniques.  
114 Petrophysical software used by leading oil companies also  
115 treat the zone parameters as constant, which have to be set  
116 before the processing of well logs. One possible solution  
117 is the use of the interval inversion technique, which al-  
118 lows the estimation of suitably chosen zone parameters  
119 and layer-thicknesses within the inversion procedure  
120 (Dobróka and Szabó 2012). The interval inversion method  
121 inverts the data set of a longer depth-interval to predict  
122 the vertical distributions of petrophysical parameters in a  
123 joint inversion procedure. In the framework of interval  
124 inversion, the model parameters including the zone pa-  
125 rameters are expanded into a series by using orthogonal  
126 polynomials as basis functions, and the expansion coeffi-  
127 cients are estimated by inversion. This approach is more  
128 stable and gives more accurate results than local inversion  
129 (Dobróka et al. 2016). For a high overdetermination (data-  
130 to-unknowns) ratio, which is responsible for the signifi-  
131 cant improvement in estimation accuracy, far fewer ex-  
132 pansion coefficients are applied as unknown parameters  
133 than inverted data. In that case, however, the vertical res-  
134 olution of the inversion method is limited. A better res-  
135 olution does not allow the incorporation of too many un-  
136 knowns. Dobróka and Szabó (2011) give an estimate to  
137 three textural parameters and four volumetric ratios in a  
138 Hungarian gas-bearing formation by using a simulated  
139 annealing based interval inversion method. Other alterna-  
140 tive methods such as factor analysis, can help reduce the  
141 number of unknowns as they allow the independent esti-  
142 mation of some petrophysical parameters such as shale

143 volume (Szabó et al. 2014) and hydraulic conductivity  
144 (Szabó 2015).

145 The zone parameters often correlate strongly to each  
146 other and volumetric parameters, which may lead to  
147 ambiguity in the inverse problem. Balázs (2015) theoret-  
148 ically shows that the amount of correlation between the  
149 zone parameters and volumetric properties increases with  
150 the number of inversion unknowns in linear inversion. On  
151 the other hand, parameter sensitivity experiments show  
152 that some zone parameters, like the saturation exponent,  
153 hardly bear influence on the observed well logs in fully  
154 saturated formations (Dobróka and Szabó 2011). Low or  
155 zero sensitivity to the saturation exponent and other zone  
156 properties may cause the failure of gradient-searching in-  
157 version methods. In addition to this problem, the linear-  
158 ized inversion procedures tend to find a solution at a local  
159 minimum of the objective function and are generally bad-  
160 ly conditioned from the numerical point of view. In such  
161 cases, when a linear inversion approach is inapplicable,  
162 one can successfully apply a global optimization method,  
163 e.g. simulated annealing or evolutionary algorithms (Sen  
164 and Stoffa 2013). Global optimization methods give both  
165 a derivative-free and a practically initial-model indepen-  
166 dent solution, while they seek the absolute extremum of  
167 the objective function. The class of genetic algorithms has  
168 been used as an effective global optimization tool for bi-  
169 ological and engineering problems and artificial intelli-  
170 gence approaches (Cranganu et al. 2015). Similar to nat-  
171 ural selection, the genetic search iteratively improves a  
172 population of artificial individuals. The population cons-  
173 ists of a number of individuals each representing one  
174 feasible solution in the model space. In geophysical inver-  
175 sion, each model parameter is coded into a chromosome,  
176 the basic elements of which, called genes, are randomly  
177 exchanged and modified during the searching process. In  
178 advanced genetic algorithms, the model parameters are  
179 encoded as real numbers and the genes are randomly  
180 modified by real operations. The float-encoded genetic  
181 algorithm (FGA) assures a high resolution of the model  
182 space and a relatively fast solution (Michalewicz 1992).

183 An FGA meta-algorithm-assisted EGS inversion meth-  
184 od, named as genetic meta-algorithmic inversion (GMI),  
185 is suggested for the simultaneous estimation of volumetric  
186 parameters and physical properties of clay and matrix  
187 components (i.e. zone parameters) using engineering geo-  
188 physical sounding data. The originally underdetermined  
189 EGS inverse problem is solved in two overdetermined  
190 inversion phases. In the inner loop of GMI, the volumetric  
191 parameters are locally estimated by a linearized inversion  
192 algorithm, whereas the zone parameters are determined by  
193 the FGA meta-algorithm in the outer loop. The GMI as-  
194 sures the best fit between the measured and calculated  
195 data and gives a reliable solution practically independent

196 of the initial model. Therefore, laboratory information on  
 197 zone parameters is unnecessary in this stage of interpreta-  
 198 tion. The GMI is numerically tested using engineering  
 199 geophysical sounding logs observed in a Hungarian un-  
 200 saturated loessy-sandy formation to confirm the feasibility  
 201 of the proposed inversion workflow.

202 **Materials and methods**

203 **Forward problem**

204 In the petrophysical characterization of unsaturated  
 205 (clastic) sediments, the rock matrix is assumed to be  
 206 composed of coarse and fine grain components and the  
 207 pore-space is occupied by freshwater and some amount  
 208 of air. In the GMI procedure, the fractional volumes of  
 209 water ( $V_w$ ), air ( $V_a$ ), clay ( $V_{cl}$ ) and sand ( $V_{sd}$ ) are calcu-  
 210 lated locally at a given depth, while the matrix and clay  
 211 properties are estimated as constant for the entire length  
 212 of a drill hole. From the inversion results, one can de-  
 213 rive the hydraulic conductivity (Nyári et al. 2010) and  
 214 other important geotechnical parameters, e.g. undrained  
 215 shear strength (Shin and Kim 2011) and dry density  
 216 (Szabó 2012).

217 In the forward modeling process, theoretical EGS logs are  
 218 calculated from the known values of model parameters, which  
 219 are adjusted to observed data by inversion. The input of the  
 220 inversion procedure is composed of natural gamma-ray inten-  
 221 sity (GR), bulk density ( $\rho_b$ ), neutron-porosity ( $\Phi_N$ ), and resis-  
 222 tivity ( $R$ ) logs. In shallow sediments, the nuclear parameters  
 223 are calculated by the response functions suggested by Drahos  
 224 (2005) and Szabó et al. (2012), while the resistivity is calcu-  
 225 lated by the model of De Witte (1955)  
 226

229 
$$GR = V_{cl}GR_{cl} + V_{sd}GR_{sd} \quad (1)$$

232 
$$\rho_b = V_w\rho_w + V_{cl}\rho_{cl} + V_{sd}\rho_{sd} \quad (2)$$

235 
$$\Phi_N = V_w\Phi_{N,w} + V_{cl}\Phi_{N,cl} + V_{sd}\Phi_{N,sd} \quad (3)$$

238 
$$R = (V_w + V_a + V_{cl})^{-m} \left( \frac{V_{cl}/(V_w + V_{cl})}{R_{cl}} + \frac{1 - [V_{cl}/(V_w + V_{cl})]}{R_w} \right)^{-1} \quad (4)$$

238 
$$\left( \frac{V_w + V_{cl}}{V_w + V_a + V_{cl}} \right)^{-2}$$

238 
$$V_w + V_a + V_{cl} + V_{sd} = 1 \quad (5)$$

239 where the zone parameters are gamma-ray intensity in sand  
 241 ( $GR_{sd}$ ) and clay ( $GR_{cl}$ ), density of water ( $\rho_w$ ), sand ( $\rho_{sd}$ ) and  
 242 clay ( $\rho_{cl}$ ), neutron-porosity of water ( $\Phi_{N,w}$ ), sand ( $\Phi_{N,sd}$ ) and  
 243 clay ( $\Phi_{N,cl}$ ), resistivity of water ( $R_w$ ) and clay ( $R_{cl}$ ), and the  
 244 cementation exponent ( $m$ ). Equation (5) represents the materi-  
 245 al balance in the soil, which derives one of the volumetric  
 246 parameters from the others.

**Estimation of volumetric rock properties**

In the local inversion phase (inner loop) of the GMI, the frac-  
 tional volume of sand, water and clay is estimated in each  
 depth separately. The air volume is estimated outside the in-  
 version procedure using Eq. (5). The column vector of EGS  
 data observed in a given depth is

$$\mathbf{d}^{(obs)} = [GR^{(obs)}, \rho_b^{(obs)}, \Phi_N^{(obs)}, R^{(obs)}]^T \quad (6)$$

where T denotes the symbol of matrix transpose. The model  
 vector of the inverse problem defined at the same depth is

$$\mathbf{m} = [V_w, V_{cl}, V_{sd}]^T \quad (7)$$

The theoretical value of the EGS data “measured” by the  $k$ -  
 th probe is given by the forward modeling procedure using the  
 relevant choice of Eqs. (1)–(4)

$$d_k^{(cal)} = f_k(V_w, V_{cl}, V_{sd}, \mathbf{p}) \quad (8)$$

where  $\mathbf{p}$  is the vector of zone parameters ( $k = 1, \dots, 4$ ). In the  
 inner loop of the GMI, the zone parameters are assumed to be  
 fixed as constant and a set of marginally overdetermined in-  
 verse problems (as having four data against three unknowns)  
 is solved along the drill hole, which has an unique solution.  
 Because of Eq. (4), the set of probe response functions  $\mathbf{f}$  is  
 nonlinear; thus, the nonlinear inverse problem is usually line-  
 arized (Menke 1984). The linear approximation of data vs.  
 model relation is  $\mathbf{d}^{(cal)} = \mathbf{J}\mathbf{m}$ , where  $\mathbf{J}$  is the 4-by-3 Jacobi’s  
 matrix including the partial derivatives of EGS data with re-  
 spect to the model parameters given in Eq. (7). The distance  
 between the measured and calculated data normalized to the  
 data variances as a measure of instrument uncertainty is given  
 in the 4-by-1 deviation vector  $\mathbf{e}$ . The objective function of the  
 inverse problem is

$$E = \|\mathbf{e}\|_2^2 + \varepsilon^2 \|\mathbf{m}\|_2^2 = \min \quad (9)$$

where  $\varepsilon^2$  is a positive regularization parameter used for stabi-  
 lizing the solution of the ill-posed inverse problem. If one has  
 no prior information on the data variances, the deviation error  
 $\mathbf{e}$  can be normalized by the observed data to take the relative  
 importance of each data type into consideration in the inver-  
 sion procedure. The actual model is refined until the best fit  
 between the measured and calculated data is achieved. The  
 vector of model parameters is continuously improved by  
 $\mathbf{m} = \mathbf{m}_0 + \delta\mathbf{m}$  in an iterative procedure, where  $\mathbf{m}_0$  is the initial  
 model. The model correction vector  $\delta\mathbf{m}$  is estimated by the  
 damped least squares method (DLSQ) suggested by  
 Marquardt (1959)

$$\delta\mathbf{m} = (\mathbf{J}^T \mathbf{J} + \varepsilon^2 \mathbf{I})^{-1} \mathbf{J}^T \delta\mathbf{d} \quad (10)$$

293 where  $\delta \mathbf{d}$  is the difference between the measured and actually  
 294 computed EGS data vector and  $\mathbf{I}$  is the unity matrix.

295 The EGS inversion method allows the checking of the  
 296 quality of the estimated model. The covariance matrix of the  
 297 model parameters estimated by a linearized inversion method  
 298 can be related to the data covariance matrix including the  
 299 variances of observed data

$$\text{covm} = \mathbf{F}^{-1} \text{covd}^{(\text{obs})} (\mathbf{F}^{-1})^T \quad (11)$$

300 where  $\mathbf{F}^{-1}$  is the generalized inverse matrix of the DLSQ  
 302 method (Menke 1984). The estimation error of volumetric  
 303 parameters is calculated as the square root of variances obtain-  
 304 ed in the main diagonal of  $\text{cov m}$ . The reliability of inversion  
 305 results can be quantified via the Pearson's correlation matrix  
 306 ( $\text{corr m}$ ) derived from Eq. (11). One can use the following  
 307 scalar for the measure of average correlation

$$S(\mathbf{m}) = \left\{ \frac{1}{M(M-1)} \sum_{u=1}^M \sum_{v=1}^M [(\text{corr}\mathbf{m})_{uv} - \delta_{uv}]^2 \right\}^{1/2} \quad (12)$$

308 where  $\delta$  denotes the Kronecker delta, and  $M$  is the number of  
 310 model parameters. The solution is considered to be reliable,  
 311 when the estimated three fractional volumes correlate poorly.  
 312 In opposite cases, high correlation causes ambiguity, which  
 313 prevents the reliable determination of the individual param-  
 314 eters by an inversion procedure.

### 315 Estimation of zone parameters

316 The global optimization phase (outer loop) of GMI provides a  
 317 heuristic search for the unknown zone parameters. In the FGA  
 318 inversion meta-algorithm, only the zone parameters are up-  
 319 dated, whereas the volumetric properties preliminary estimat-  
 320 ed in the inner loop of iterations are treated as fixed param-  
 321 eters. The model vector is composed of the matrix and clay  
 322 properties being the unknowns of the inverse problem  
 323

$$\tilde{\mathbf{p}} = [\text{GR}_{\text{cl}}, \text{GR}_{\text{sd}}, R_{\text{cl}}, \rho_{\text{cl}}, \rho_{\text{sd}}, \Phi_{N,\text{cl}}]^T \quad (13)$$

324 the constant values of which are estimated for the entire pro-  
 326 cessing interval. To achieve this, all data collected from the  
 327 drill hole are integrated in one data vector

$$\tilde{\mathbf{d}}^{(\text{obs})} = [\mathbf{d}_1^{(\text{obs})}, \mathbf{d}_2^{(\text{obs})}, \dots, \mathbf{d}_i^{(\text{obs})}, \dots, \mathbf{d}_N^{(\text{obs})}]^T \quad (14)$$

328 where  $N$  is the total number of processed depths. In the genetic  
 330 search, the lower and upper bounds of zone parameters are  
 331 first initialized. A number of randomly generated models of  
 332 zone properties as individuals is simultaneously tested during  
 333 the optimization process, in which those having parameters  
 334 out of the physical range are effectively rejected. In the first

phase of the GMI, a set of DLSQ inversion runs are executed  
 by fixed values of zone parameters for the determination of the  
 depth distribution of volumetric parameters (inner loop of  
 GMI). Then, the updated values of fractional volumes are  
 fixed, and the zone parameters are re-calculated by fitting  
 the observed and predicted data by the FGA process (outer  
 loop of GMI). The two phases of the GMI are repeated until a  
 stop criterion is met.

In the outer loop of GMI, a population of model vectors  $\tilde{\mathbf{p}}_j$   
 ( $j = 1, 2, \dots, P$ , where  $P$  is the population size) is gradually im-  
 proved to minimize the misfit between the observed data given  
 in Eq. (14) and those calculated using Eq. (8). For data  
 prediction, the same probe response functions given in Eqs.  
 (1)–(4) are used as in local inversion. The chromosome of an  
 individual is built up from the model parameters of Eq. (13).  
 According to the Darwinian theory of evolution, the fittest  
 individuals survive and reproduce, while others disappear  
 from the population over time. In this study, the fitness of  
 the  $j$ -th model is calculated from the normalized data deviation  
 along the entire length of the drill hole

$$F(\tilde{\mathbf{p}}_j) = - \left[ \frac{1}{NK} \sum_{i=1}^N \sum_{k=1}^K \left( \frac{\tilde{d}_{ik}^{(\text{obs})} - f_k(\mathbf{m}_i, \tilde{\mathbf{p}}_j)}{\tilde{d}_{ik}^{(\text{obs})}} \right)^2 \right]^{1/2} \quad (15)$$

where  $\mathbf{m}_i$  is the vector of volumetric parameters fixed at  
 the  $i$ -th depth ( $i = 1, 2, \dots, N$ ) and  $K$  is the number of ap-  
 plied probes. The solution of the optimization problem is  
 to be found at  $F(\tilde{\mathbf{p}}) = \max$ . The value of fitness multi-  
 plied by  $-100$  characterizes the relative distance between  
 the measured and calculated EGS logs in percent. Next, a  
 suitable combination of real genetic operations is used to  
 increase the average fitness of subsequent generations. In  
 order to get a quick solution and best resolution, floating-  
 point genetic operations such as selection, crossover and  
 mutation are implemented (Houck et al. 1995).

At first the fittest individuals are selected for reproduction.  
 In this study, the mating of individuals is performed by tour-  
 nament selection. In the selection process, a number of indi-  
 viduals are randomly chosen from the population, with re-  
 placement, and the fittest ones are copied into the new popu-  
 lation. This procedure is repeated until  $P$  number of individ-  
 uals have been selected. This approach is probability-free un-  
 like other selection methods, e.g. roulette wheel or ranking  
 operations (Razali and Geraghty 2011). The number of tour-  
 naments as a control parameter is set to ensure the develop-  
 ment of convergence of the genetic search. Less adaptable  
 individuals have a smaller chance to be selected for the next  
 generation if this tournament size is large. In the next step, a  
 pair of individuals ( $\tilde{\mathbf{p}}_1$  and  $\tilde{\mathbf{p}}_2$ ) is chosen from the actual  
 population that had undergone the selection process and some

383 amount of genetic information is exchanged between them.  
 384 By the use of simple or multi-point crossover, the model vectors  
 385 are divided into two or more segments, the genes of which  
 386 are exchanged between the crossover points to get new individuals.  
 387 The heuristic crossover extrapolates two individuals  
 388 as follows  
 389

$$\begin{aligned} \tilde{\mathbf{p}}_1 &= \tilde{\mathbf{p}}_1 + \alpha(\tilde{\mathbf{p}}_1 - \tilde{\mathbf{p}}_2) \\ \tilde{\mathbf{p}}_2 &= \tilde{\mathbf{p}}_1 \end{aligned} \quad (16)$$

390 where  $\alpha$  is a random number generated from  $U(0,1)$ . It is  
 392 assumed that the fitness value of  $\tilde{\mathbf{p}}_1$  is higher than that of  
 393  $\tilde{\mathbf{p}}_2$ . If any value of  $\tilde{\mathbf{p}}_1$  is out of bounds, a new random number  
 394 is generated and Eq. (16) is recalculated. After a certain number  
 395 of failures, the new values of model parameters are set to  
 396 equal the old ones. The third genetic operation is a uniform  
 397 mutation. For the mutation process, the model vector  $\tilde{\mathbf{p}}_1$  is  
 398 selected and its  $l_0$ -th parameter is substituted with a random  
 399 floating-point number ( $\beta$ ) generated from its pre-defined  
 400 range  
 401

$$\tilde{\mathbf{p}}'_1 = \begin{cases} \beta, & \text{if } l = l_0 \\ \tilde{\mathbf{p}}_{1,l}, & \text{otherwise} \end{cases} \quad (17)$$

402 where  $\tilde{\mathbf{p}}'_1$  is the mutated individual. The selection and the  
 404 preceding genetic operations (Eqs. 16–17) are applied in successive  
 405 generations until a termination criterion is met. An elitism-based  
 406 reproduction can be optionally used, which

preserves the fittest individual(s) of the previous generation  
 and replaces the weakest with them in the next generation  
 (Bijani et al. 2012). The stop criterion is defined either as the  
 maximum number of generations or a specified threshold in  
 the distance between the measured and calculated data. In the  
 last generation, the model vector with maximum fitness is  
 regarded as the solution of the global optimization problem.  
 The estimation error of a zone parameter is calculated as the  
 standard deviation of its values obtained for different individuals  
 in the last generation.

## Feasibility results

### Geological setting

The GMI is tested in the Bataapati (Üveghuta) site, South-West Hungary (Fig. 2a). Ground geophysical surveys were previously carried out for establishing a nuclear waste repository in the igneous bedrock (Vértesy et al. 2004). The aim of geophysical measurements in the shallow unconsolidated sediments was to detect neotectonic events by tracing horizons connected with soils and explore local hydrogeological conditions. The loessy-sandy formation is deposited on a partially weathered granite basement, where the water table is situated approximately at the top of the granite. The EGS logs were measured in the upper 20–30 m of the loose unsaturated formation in seven drill holes (H4–H10) located 50 m apart from each other along a 300-m-long profile (Fig. 2b). The zone

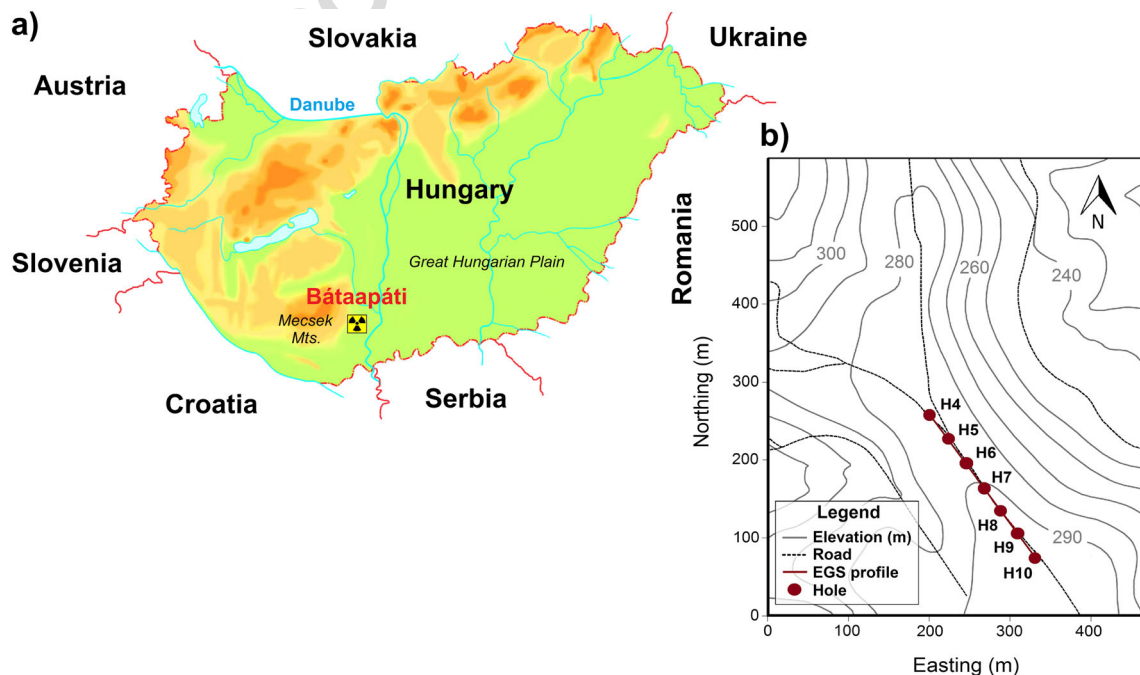


Fig. 2 Location map of the studied area: a Bataapati well site in South West Hungary, b topographic map and the profile of the investigated drill holes

432 parameters in Eqs. (1)–(4) other than clay and matrix proper- 470  
 433 ties are given from the literature (Drahos 2005), i.e.  $R_w = 12$  471  
 434 ohmm,  $m = 1.7$ ,  $\rho_w = 1.0 \text{ g/cm}^3$ ,  $\Phi_{N,w} = 1.0 \text{ v/v}$ ,  $\Phi_{N,sd} = 0 \text{ v/v}$ . 472  
 435 In Eqs. (2)–(3), the air volume is not included, because the 473  
 436 mass density and neutron-porosity of air are set to zero. 474

437 **Single borehole application**

438 In a one-dimensional (1D) application of the GMI, the ver- 475  
 439 tical distribution of water, clay and quartz volumes and the 476  
 440 constant values of matrix and clay properties are simulta- 477  
 441 neously estimated in drill hole H4 (Fig. 2b). The input of 478  
 442 the inversion procedure is composed of the GR,  $\rho_b$ ,  $\Phi_N$ ,  $R$  479  
 443 logs measured with a sampling interval of 0.1 m. Table 1 480  
 444 shows a moderate correlation between the EGS measure- 481  
 445 ment types on average. The mean of Pearson’s correlation 482  
 446 coefficients calculated by Eq. (12) is  $S = 0.55$ . The stron- 483  
 447 gest correlation is indicated between the resistivity and po- 484  
 448 rosity logs. The uncertainty of EGS data represented by the 485  
 449 data variances in Eq. (11) are chosen from Drahos (2005) 486  
 450 such as  $\sigma_{GR}^2 = 0.05 \text{ kcpm}^2$ ,  $\sigma_{\rho_b}^2 = 0.01 \text{ g}^2/\text{cm}^6$ , 487  
 451  $\sigma_{\Phi_N}^2 = 2.5 \cdot 10^{-3} \text{ v}^2/\text{v}^2$ ,  $\sigma_R^2 = 0.05 \text{ ohm}^2 \text{ m}^2$ . The forward 488  
 452 problem is solved using Eqs. (1)–(4) in both phases of the 489  
 453 1D GMI. 490

454 In the inner loop of iterations, the volumetric properties are 491  
 455 updated by Eq. (10), the initial values of which for each depth 492  
 456 are chosen as  $V_{w,0} = 0.3 \text{ v/v}$ ,  $V_{sd,0} = 0.4 \text{ v/v}$ ,  $V_{cl,0} = 0.15 \text{ v/v}$ . 493  
 457 The air volume is directly derived from the EGS inversion 494  
 458 results using Eq. (5). The optimal solution is found after 10 495  
 459 iteration steps in each depth. The regularization factor in Eq. 496  
 460 (10) is chosen as  $\varepsilon^2 = 0$ , which shows a stable linearized in- 497  
 461 version process. At the end of the local inversion phase, the 498  
 462 1D GMI is switched to the FGA searching (outer) loop. The 499  
 463 fractional volumes estimated in the last iteration of local in- 500  
 464 version are fixed, and the start population with 30 individuals 501  
 465 is initialized (Fig. 3a). The search domain of the matrix and 502  
 466 clay properties is listed in Table 2. The fitness of individuals 503  
 467 is calculated by Eq. (15), which has local maxima at certain 504  
 468 selected values of zone parameters (Fig. 3c–d). The genetic 505  
 469 operators including tournament selection, heuristic crossover 506

t1.1 **Table 1** Pearson’s correlation matrix of engineering geophysical sounding logs measured in drill hole H4

t1.2		GR	$\rho_b$	$\Phi_N$	$R$
t1.3	GR	1	0.23	0.11	−0.29
t1.4	$\rho_b$	0.23	1	0.65	−0.73
t1.5	$\Phi_N$	0.11	0.65	1	−0.83
t1.6	$R$	−0.29	−0.73	−0.83	1

GR gamma-ray intensity;  $\rho_b$  bulk density;  $\Phi_N$  neutron-porosity;  $R$  resistivity logs

and uniform mutation are used to find the optimal values of 470  
 zone parameters. The control parameters of FGA are chosen 471  
 as tournament size (200), crossover retry (50) and mutation 472  
 probability (0.05). An elitism-based reproduction is per- 473  
 formed, as the vector of zone parameters with the maximum 474  
 fitness is automatically copied into the next generation. After 475  
 each local inversion loop including 10 iterations, the FGA 476  
 procedure runs over 1,000 generations. The total number of 477  
 iterations of the 1D GMI is set to 10. As a result of the com- 478  
 bined use of linear and global inversion methods, the relative 479  
 distance between the measured and calculated data decreases 480  
 continuously (Fig. 3b). In the first step of 1D GMI, the relative 481  
 data distance is 39%, which reduces to 4% at the end of the 482  
 inversion procedure. The measured and calculated EGS logs 483  
 as well as the optimal values of volumetric parameters can be 484  
 found in Fig. 4. The estimation errors of volumetric param- 485  
 eters calculated by Eq. (11) are obtained as  $\sigma_{V_w} = 0.6 \text{ v/v}$ , 486  
 $\sigma_{V_{sd}} = 5.4 \text{ v/v}$ ,  $\sigma_{V_{cl}} = 0.93 \text{ v/v}$  (Fig. 5). The mean correlation 487  
 between the volumetric parameters calculated by Eq. (12) is 488  
 $S = 0.51$ . As part of the inversion result, the estimated values 489  
 of zone parameters including their estimation errors are listed 490  
 in Table 2. The inversion results show stable and reliable in- 491  
 version procedure. The required CPU time of the 1D GMI 492  
 using a quad-core processor workstation is 4 min 43 s. 493

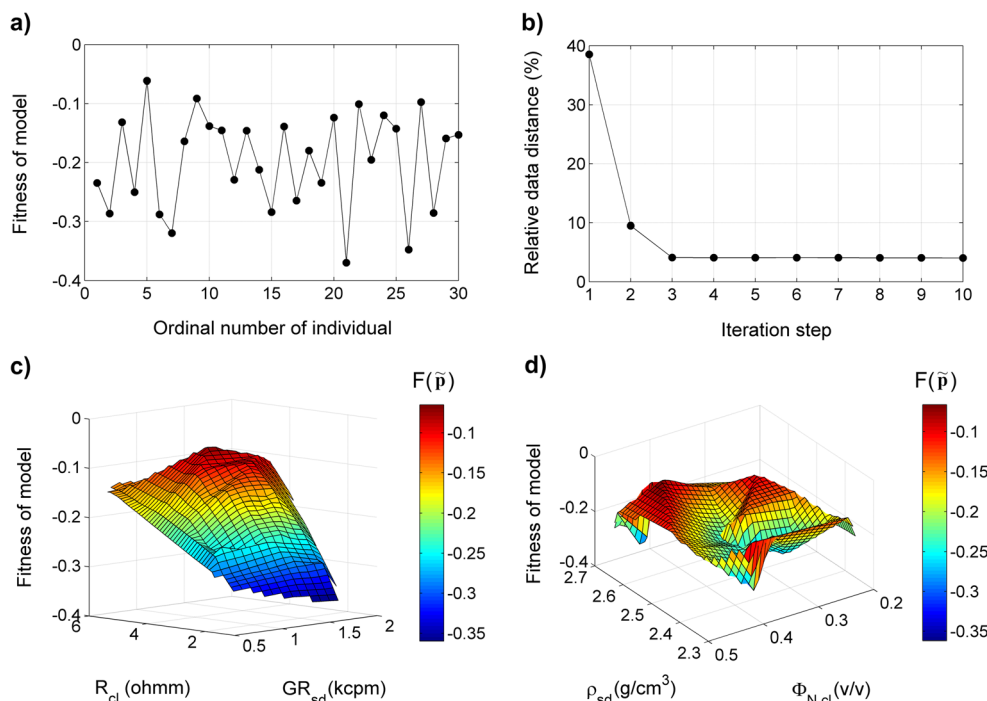
494 **Multi-borehole application**

495 The two-dimensional (2D) version of the GMI allows the 496  
 estimation of the volumetric properties and zone parameters 497  
 not only along the depth coordinate but also as a horizontal 498  
 profile of drill holes. It is assumed that the zone parameters 499  
 do not change significantly in lateral direction. Therefore, the 500  
 volumetric parameters are determined in each depth by local 501  
 inversion, whereas the zone parameters are treated as con- 502  
 stants in the whole shallow region and estimated by the 503  
 FGA procedure. The only difference between the 1D and 2D 504  
 GMIs is that the fitness of the  $j$ -th model, in the 2D case, is 505  
 calculated using the data from all drill holes 506

$$F^*(\tilde{\mathbf{p}}_j) = - \left[ \frac{1}{HKN^*} \sum_{h=1}^H \sum_{k=1}^K \sum_{i=1}^{N_h} \left( \frac{\tilde{d}_{hki}^{(obs)} - f_k(\mathbf{m}_{hi}, \tilde{\mathbf{p}}_j)}{d_{hki}^{(obs)}} \right)^2 \right]^{1/2} \tag{18}$$

where  $\mathbf{m}_{hi}$  is the vector of volumetric parameters fixed at 508  
 the  $i$ -th depth in the  $h$ -th hole,  $N_h$  is the number of pro- 509  
 cessed depths in the  $h$ -th hole and  $H$  is the total number of 510  
 penetration holes. The solution of the inverse problem is to 511  
 be found at  $F^*(\tilde{\mathbf{p}}) = \max$ . In the 2D GMI, the GR,  $\rho_b$ ,  $\Phi_N$ , 512  
 $R$  logs measured in drill holes H4–H10 are simultaneously 513  
 inverted (Fig. 2b). The sampling interval is 0.1 m and the 514

**Fig. 3** Genetic meta-algorithmic inversion process in drill hole H4 **a** fitness values of individuals including the zone parameters generated in the initial population, **b** data misfit vs. iteration step during the GMI process, **c** fitness vs. clay resistivity ( $R_{cl}$ ) and gamma-ray intensity in sand ( $GR_{sd}$ ), **d** fitness vs. sand density ( $\rho_{sd}$ ) and neutron-porosity of clay ( $\Phi_{N,cl}$ )



515 lengths of drill holes are not exactly the same (the bottom  
516 is between 19.9–27.7 m). The total number of EGS data is  
517  $N^* = N_1 + N_2 + \dots + N_H = 6,972$ . The mean spread calculat-  
518 ed by Eq. (12) is  $S = 0.27$ , which shows weaker correlation  
519 between the observed physical quantities than in hole H4.  
520 This may be due to the lateral variation of lithology and  
521 data noise. The strongest correlation is indicated between  
522 the resistivity and neutron-porosity logs (Table 3). The  
523 theoretical values of EGS data are calculated using Eqs.  
524 (1)–(4), in both phases of the 2D GMI, and the same data  
525 variances are assumed as in section ‘Single borehole  
526 application’.

527 In the inner loop of iterations, the DLSQ method is used  
528 to produce the 2D interpolated sections of volumetric prop-  
529 erties (Fig. 6); note that the same control parameters are  
530 used as in section ‘Single borehole application’. In the  
531 FGA search phase, a population of model vectors (13) is

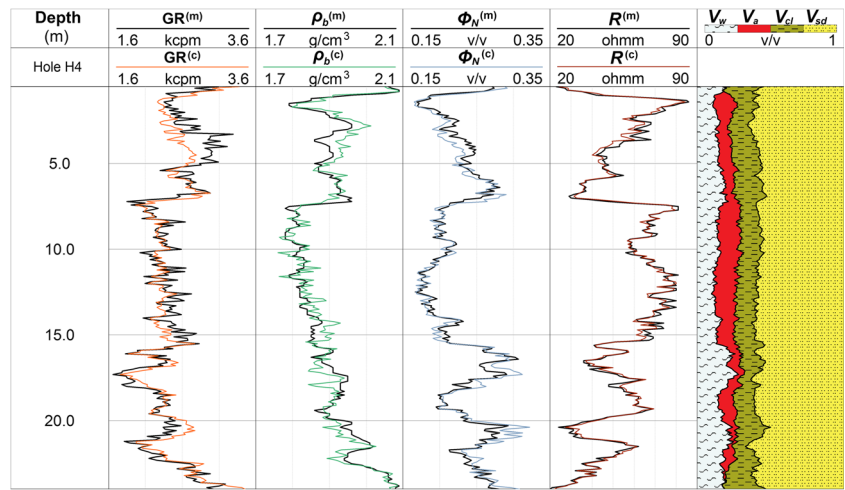
improved in 250 generations using the same genetic oper- 532  
ations as in section ‘Single borehole application’. The fitness 533  
of individuals is evaluated using Eq. (18). The esti- 534  
mated values of the matrix and clay properties are found in 535  
Table 4, the errors of which are calculated as the standard 536  
deviations of model parameters given in the last generation. 537  
At the end of the 2D GMI, the average of relative data 538  
distance decreases from 42.4 to 4.9%. The 2D distribution 539  
of relative data distance is plotted in Fig. 7a. The largest 540  
deviations are associated primarily to interpolation errors 541  
because of the different drilling depths. The quadratic mean 542  
of the estimation errors of volumetric parameters calculated 543  
by Eq. (11) is below 0.046 v/v (Fig. 7b), its average is 544  
0.038 v/v, and the mean spread of the same quantities is 545  
 $S = 0.49$ . This result also shows stable and reliable inver- 546  
sion procedure. The CPU time of the 2D GMI using a quad- 547  
core processor workstation is 8 min 41 s. 548

t2.1 **Table 2** Zone parameters  
t2.2 estimated by 1D genetic meta-  
t2.3 algorithmic inversion in drill hole  
t2.4 H4

Zone parameter	Search domain	Estimated value	Estimation error	Unit
$GR_{cl}$	8.0–12.0	8.86	0.01	kcpm
$GR_{sd}$	0–2.0	1.83	0.01	kcpm
$\rho_{cl}$	1.9–2.3	2.07	0.02	$g/cm^3$
$\rho_{sd}$	2.3–2.7	2.41	0.01	$g/cm^3$
$\Phi_{N,cl}$	0.2–0.5	0.43	0.05	v/v
$R_{cl}$	1.0–6.0	4.56	0.61	ohmm

$GR_{cl}$  and  $GR_{sd}$  gamma-ray intensity of clay and sand, respectively;  $\rho_{cl}$  and  $\rho_{sd}$  density of clay and sand, respectively;  $\Phi_{N,cl}$  neutron-porosity of water;  $R_{cl}$  resistivity of clay

**Fig. 4** Engineering geophysical sounding logs measured (m) and calculated (c) in drill hole H4 (tracks 1–4). GR is natural gamma-ray intensity,  $\rho_b$  is bulk density,  $\Phi_N$  is neutron-porosity,  $R$  is resistivity. Petrophysical parameters estimated by genetic meta-algorithmic inversion are fractional volumes of water ( $V_w$ ), air ( $V_a$ ), clay ( $V_{cl}$ ) and sand ( $V_{sd}$ ) (track 5)



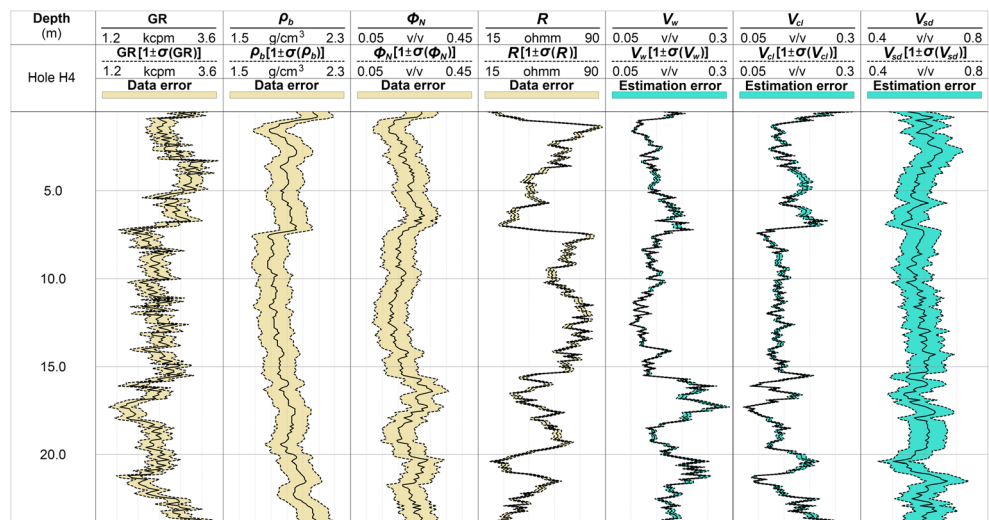
**549 Discussion**

550 The estimation of zone parameters has been one of the most  
 551 challenging task in formation evaluation. It was previously  
 552 studied that well-logging data are often insensitive to the varia-  
 553 tion of zone parameters such as tortuosity coefficient and  
 554 saturation exponent, which also show high correlation to each  
 555 other. During the inversion tests, high correlation was observed  
 556 between the resistivity of water and density parameters. Because of the problem of ambiguity, the number of  
 557 zone parameters estimated by inversion is restricted; however, these numerical tests show that the matrix and clay  
 558 properties can be simultaneously estimated with the volumetric parameters in a stable meta-algorithmic inversion  
 559 procedure. The use of global optimization is justified since there are several local maxima of the fitness function at  
 560 selected values of zone parameters. The adaptability, numerical stability and initial-model independence of the  
 561 FGA are proven to be higher than those of linearized inversion

562 methods which usually become unstable in ambiguous situa-  
 563 tions and thus give a divergent solution. On the other hand, in  
 564 the traditional local inversion approach, it is inevitably impos-  
 565 sible to find a reliable solution for the volumetric and zone  
 566 parameters together in one underdetermined inversion proce-  
 567 dure (i.e. the estimation of six zone parameters and three vol-  
 568 umetric properties— nine unknowns in total—from four data  
 569 sets).

570 The inversion results of the 1D and 2D GMIs show a  
 571 close agreement. The estimation of volumetric parameters  
 572 is made without regularization in both cases. The uncer-  
 573 tainty of the fractional volumes is proportional to that of  
 574 the input data (Fig. 5). In case of extremely noisy data sets,  
 575 the application of robust weighting procedures is advis-  
 576 able, which effectively suppress the instrument noise, es-  
 577 pecially the influence of outliers (Steiner 1991). The most  
 578 accurate parameters are the water volume and clay content,  
 579 the standard deviation of which is obtained around 1 v/v.  
 580 For a more reliable estimation of the matrix volume, it is

**Fig. 5** Quality results of 1D genetic meta-algorithmic inversion in drill hole H4. Observed engineering geophysical sounding logs and their confidence intervals (tracks 1–4). Estimated petrophysical parameters and their estimation errors (tracks 5–7) ( $\sigma$  is standard deviation)



t3.1 **Table 3** Pearson's correlation matrix of engineering geophysical sounding logs measured in drill holes H4-H10

t3.2		GR	$\rho_b$	$\Phi_N$	$R$
t3.3	GR	1	0.03	0.13	0.07
t3.4	$\rho_b$	0.03	1	-0.01	0.08
t3.5	$\Phi_N$	0.13	-0.01	1	0.63
t3.6	$R$	0.07	0.08	0.63	1

GR gamma-ray intensity;  $\rho_b$  bulk density,  $\Phi_N$  neutron-porosity;  $R$  resistivity logs

586 necessary to include new measurement types, the number of  
 587 which is relatively limited in this stage of the EGS technology.  
 588 New directions of tool development aim to measure such pa-  
 589 rameters that give information on the pore-space distribution  
 590 and the type and level of soil contamination. The obtained

values and estimation errors of zone parameters also con- 591  
 firm the feasibility of both the 1D and 2D GMI. In compar- 592  
 ing the estimation results, very similar results are giv- 593  
 en for the resistivity of clay, which is a basic parameter 594  
 of the dual water model. Much larger differences are 595  
 obtained for the density of quartz and the neutron- 596  
 porosity of clay, which will be studied in the future using 597  
 different real data sets. The estimated values of zone 598  
 parameters show a close agreement also with the results 599  
 of Drahos (2005). The CPU time of the GMI is accept- 600  
 able, which can be further improved by using more pow- 601  
 erful workstations or by using the very fast simulated re- 602  
 annealing, as a quick global optimization method prop- 603  
 osed by Ingber (1989) in the outer loop of the GMI. 604

### Conclusions 605

A new inversion strategy assisted by evolutionary compu- 606  
 tation is proposed for evaluating the petrophysical prop- 607  
 erties of the shallow unsaturated zone. The novel ap- 608  
 proach named GMI combines the estimation of volumetric 609  
 rock properties and zone parameters for improving the 610  
 reliability of hydrogeological interpretation. By the inver- 611  
 sion procedure, the physical properties of clay and matrix 612  
 are estimated from an objective source. By using an adap- 613  
 tive genetic algorithm, the inversion process is practically 614  
 initial-model independent, which does not require the ini- 615  
 tial value of the zone parameters. There is no need for 616  
 laboratory data for the inversion process; they are only 617  
 necessary for the initialization of FGA to set a possible 618  
 range of zone parameters. Another advantage of the GMI 619  
 is that with more accurate definition of zone parameters, 620  
 the response functions of the forward problem are also 621  
 automatically calibrated. The local inversion phase of 622  
 the GMI provides both a fast solution and a high vertical 623  
 resolution for the volumetric rock model, while the global 624  
 optimization process provides a derivative-free solution 625  
 for matrix and fluid parameters by effectively avoiding 626  
 the ambiguity domains of correlated zone parameters. 627  
 The latter computes the estimation error of the zone pa- 628  
 rameters from the entire population. By incorporating the 629  
 data measured on core samples, the domains of zone pa- 630  
 rameters can be further constrained or the inversion re- 631  
 sults can be confirmed with the laboratory measurements. 632

The GMI hopefully becomes a useful tool not only in 633  
 hydrogeophysical but also in oilfield well-logging applica- 634  
 tions where a large number of zone parameters affect the 635  
 outcome of the evaluation of hydrocarbon reservoirs. 636  
 Future research will extend the GMI to 3D applications, 637  
 which will further improve the hydrogeological model of 638  
 near-surface sediments. The optimization tool used in the 639  
 inversion procedure will be made robust by using 640

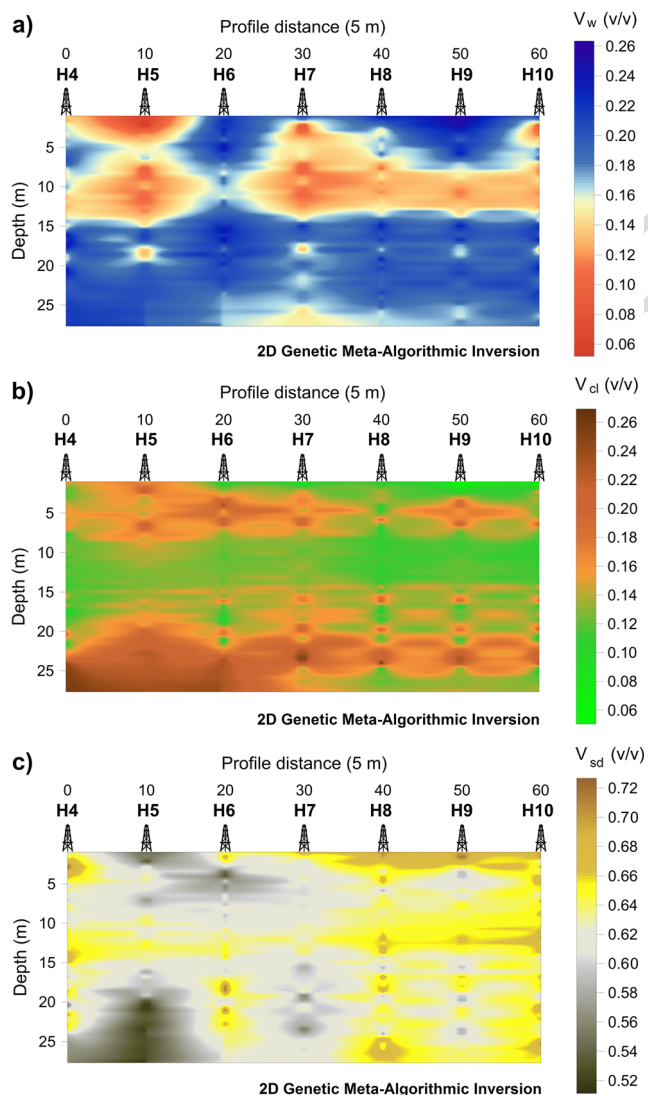


**Fig. 6** Results of 2D genetic meta-algorithmic inversion in drill holes H4-H10: **a** water volume ( $V_w$ ) estimated by 2D GMI, **b** clay volume ( $V_{cl}$ ) estimated by 2D GMI, **c** sand volume ( $V_{sd}$ ) estimated by 2D GMI

t4.1 **Table 4** Zone parameters  
t4.2 estimated by 2D genetic meta-  
t4.3 algorithmic inversion in drill  
t4.4 holes H4–H10

Zone parameter	Search domain	Estimated value	Estimation error	Unit
$GR_{cl}$	8.0–12.0	8.02	0.17	kcpm
$GR_{sd}$	0–2.0	1.98	0.01	kcpm
$\rho_{cl}$	1.9–2.3	1.97	0.03	$g/cm^3$
$\rho_{sd}$	2.3–2.7	2.31	0.01	$g/cm^3$
$\Phi_{N,cl}$	0.2–0.5	0.33	0.01	v/v
$R_{cl}$	1.0–6.0	4.19	0.49	ohmm

$GR_{cl}$  and  $GR_{sd}$  gamma-ray intensity of clay and sand, respectively;  $\rho_{cl}$  and  $\rho_{sd}$  density of clay and sand, respectively;  $\Phi_{N,cl}$  neutron-porosity of water;  $R_{cl}$  resistivity of clay

641 statistically efficient weighting procedures, e.g. Cauchy or  
642 Steiner weights, to exclude the harmful effect of outliers  
643 and enable a more robust processing of non-Gaussian data.  
644 The output of inverse modeling can be used fruitfully in the  
645 factor analysis of the same EGS logs. The statistical factors  
646 can be applied for a more reliable estimation of water saturation  
647 and the derivation of hydraulic conductivity. In a  
648 reverse process, one may increase the overdetermination of  
649 the inverse problem by using the factor analysis-derived  
650 water saturation as a fixed parameter during the inversion  
651 process. The combination of the GMI with the aforementioned  
652 interval inversion method would make it possible to  
653 further improve the estimation accuracy of volumetric parameters  
654 and to determine the layer-thicknesses in an automated  
655 inversion procedure. The latter can also be extended

to multi-borehole applications to locate the soil boundaries  
and to detect the lateral variation of the water table.

**Acknowledgements** The research was carried out within the GINOP-2.3.2-15-2016-00031 “Innovative solutions for sustainable groundwater resource management” project of the Faculty of Earth Science and Engineering of the University of Miskolc in the framework of the Széchenyi 2020 Plan. The author thanks Professor Mihály Dobróka, University of Miskolc, Associate Professor Dezső Drahos, Roland Eötvös University of Budapest, and János Stickel from Elgoscar-2000 Ltd. for the long-term scientific cooperation.

**Funding Information** The research was funded by the European Union and co-financed by the European Structural and Investment Funds.

**References**

Balázs L (2015) Inversion of well logging measurements with a constant interval parameter. *Geosci Eng* 4(6):93–104

Bijani R, Ponte Neto CF, Martins SS, Travassos JM (2012) 2-D tomography of first-arrivals using the genetic algorithm with elitism. *SEG Technical Program Expanded Abstracts 2012*:1–6. <https://doi.org/10.1190/segam2012-0489.1>

Butler JJR (2005) Hydrogeological methods for estimation of spatial variations in hydraulic conductivity. In: Rubin Y, Hubbard SS (eds) *Hydrogeophysics*. Springer, Dordrecht, The Netherlands, pp 23–58

Cranganu C, Luchian H, Breaban ME (2015) *Artificial intelligent approaches in petroleum geosciences*. Springer, Heidelberg, Germany

De Witte L (1955) A study of electric log interpretation methods in shaly formations. *Petroleum Trans AIME* 204:103–110

Dobróka M, Szabó NP (2011) Interval inversion of well-logging data for objective determination of textural parameters. *Acta Geophys* 59(5): 907–934. <https://doi.org/10.2478/s11600-011-0027-z>

Dobróka M, Szabó NP (2012) Interval inversion of well-logging data for automatic determination of formation boundaries by using a float-encoded genetic algorithm. *J Pet Sci Eng* 86–87:144–152. <https://doi.org/10.1016/j.petrol.2012.03.028>

Dobróka M, Szabó NP, Tóth J, Vass P (2016) Interval inversion approach for an improved interpretation of well logs. *Geophysics* 81(2): D163–D175. <https://doi.org/10.1190/GEO2015-0422.1>

Drahos D (2005) Inversion of engineering geophysical penetration sounding logs measured along a profile. *Acta Geodaet Geophys* 40(2):193–202. <https://doi.org/10.1556/AGeod.40.2005.2.6>

Fejes I, Jóna E (1990) The engineering geophysical sounding method: principles, instrumentation, and computerised interpretation. In: Ward SH (ed) *Geotechnical and environmental geophysics, environmental and groundwater, vol 2*. SEG, Tulsa, OK, pp 321–331

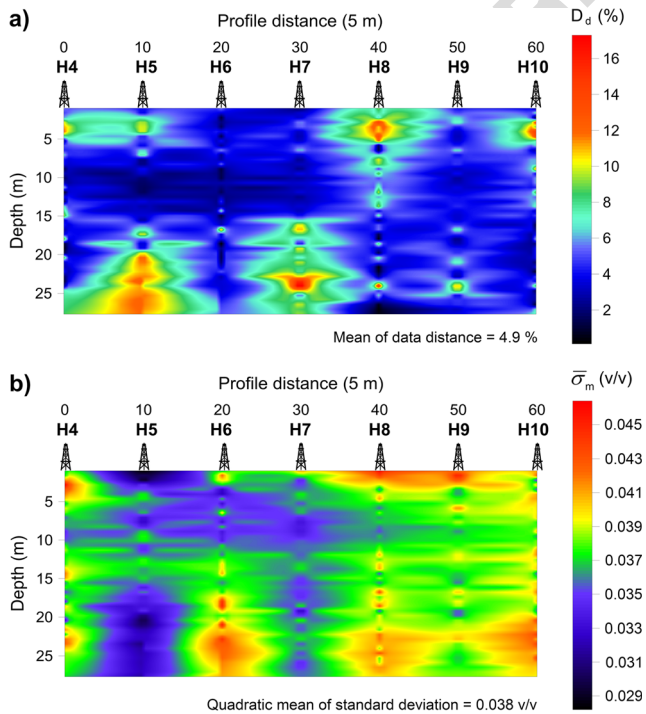


**Fig. 7** Quality results of 2D genetic meta-algorithmic inversion in drill holes H4–H10: **a** 2D section of relative data distance ( $D_d$ ) between observed and calculated engineering geophysical sounding logs, **b** 2D section of average estimation error of fractional volumes ( $\bar{\sigma}_m$ )

- 702 Houck CR, Joines J, Kay M (1995) A genetic algorithm for function  
703 optimization: a MATLAB implementation. NCSU-IE technical re-  
704 port 95–09. North Carolina State University, Raleigh, NC, pp 1–14
- 705 Ingber AL (1989) Very fast simulated re-annealing. *Math Comput Model*  
706 12(8):967–973. [https://doi.org/10.1016/0895-7177\(89\)90202-1](https://doi.org/10.1016/0895-7177(89)90202-1)
- 707 Kirsch R (2006) *Groundwater geophysics: a tool for hydrogeology*.  
708 Springer, Heidelberg, Germany
- 709 Marquardt DW (1959) Solution of non-linear chemical engineering  
710 models. *Chem Eng Prog* 55(6):65–70
- 711 Menke W (1984) *Geophysical data analysis: discrete inverse theory*.  
712 Academic, San Diego
- 713 Michalewicz Z (1992) *Genetic algorithms + data structures = evolution*  
714 *programs*. Springer, Heidelberg, Germany
- 715 Narayan JP, Yadav L (2006) Application of adaptive processing tech-  
716 nique for the inversion of open hole logs recorded in oil fields of  
717 Indian basins. In: 6th International Conference & Exposition on  
718 petroleum geophysics “Kolkata 2006”. Society of Petroleum  
719 Geophysicists, Uttarakhand, India, pp 505–512
- 720 Razali NM, Geraghty J (2011) Genetic algorithm performance with dif-  
721 ferent selection strategies in solving TSP. In: Proceedings of the  
722 World Congress on Engineering 2011, vol II, London, July 2011,  
723 pp 1–6
- 724 Schulmeister MK, Butler JJ, Healey JM, Zheng L, Wysocki DA, McCall  
725 GW (2003) Direct-push electrical conductivity logging for high-  
726 resolution hydrostratigraphic characterization. *Ground Water*  
727 *Monit Remediation* 23(2):52–62. [https://doi.org/10.1111/j.1745-](https://doi.org/10.1111/j.1745-728)  
728 [6592.2003.tb00683.x](https://doi.org/10.1111/j.1745-728)
- 729 Sen MK, Stoffa PL (2013) *Global optimization methods in geophysical*  
730 *inversion*. Cambridge University Press, Cambridge, UK
- 731 Shin YJ, Kim D (2011) Assessment of undrained shear strength based on  
732 cone penetration test (CPT) for clayey soils. *KSCE J Civ Eng* 15(7):  
733 1161–1166. <https://doi.org/10.1007/s12205-011-0808-6>
- 734 Steiner F (1991) The most frequent value: introduction to a modern con-  
735 ception of statistics. Academic, Budapest
- 736 Szabó NP (2012) Dry density derived by factor analysis of engineering  
737 geophysical sounding measurements. *Acta Geodaet Geophys* 47(2):  
738 161–171. <https://doi.org/10.1556/AGeod.47.2012.2.5>
- 739 Szabó NP (2015) Hydraulic conductivity explored by factor analysis of  
740 borehole geophysical data. *Hydrogeol J* 23(5):869–882. [https://doi.](https://doi.org/10.1007/s10040-015-1235-4)  
741 [org/10.1007/s10040-015-1235-4](https://doi.org/10.1007/s10040-015-1235-4)
- 742 Szabó NP, Dobróka M, Drahos D (2012) Factor analysis of engineering  
743 geophysical sounding data for water saturation estimation in shallow  
744 formations. *Geophysics* 77(3):WA35–WA44. [https://doi.org/10.](https://doi.org/10.1190/geo2011-0265.1)  
745 [1190/geo2011-0265.1](https://doi.org/10.1190/geo2011-0265.1)
- 746 Szabó NP, Dobróka M, Turai E, Szűcs P (2014) Factor analysis of bore-  
747 hole logs for evaluating formation shaliness: a hydrogeophysical  
748 application for groundwater studies. *Hydrogeol J* 22(3):511–526.  
749 <https://doi.org/10.1007/s10040-013-1067-z>
- 750 Szalai S, Lempenger I, Metwaly M, Kis A, Wesztergom V, Szokoli K,  
751 Novák A (2015) Increasing the effectiveness of electrical resistivity  
752 tomography using  $\gamma 11n$  configurations. *Geophys Prospect* 63(2):  
753 508–524. <https://doi.org/10.1111/1365-2478.12215>
- 754 Vértessy L, Fancsik T, Fejes I, Gulyás Á, Hegedűs E, Kovács Acs, Kovács  
755 P, Kiss J, Madarasi A, Sörös L, Szabó Z, Tóth Z (2004) Ground-  
756 based geophysical surveys at the Bataapáti (Üveghuta) Site and in its  
757 vicinity. In: Annual Report of the Geological Institute of Hungary  
758 2003, Budapest, pp 239–256
- 759 Walsh D, Turner P, Grunewald E, Zhang H, Butler JJ, Reboulet E,  
760 Knobbe S, Christy T, Lane JW, Johnson CD, Munday T,  
761 Fitzpatrick A (2013) A small-diameter NMR logging tool for  
762 groundwater investigations. *Groundwater* 51(6):914–926. [https://](https://doi.org/10.1111/gwat.12024)  
763 [doi.org/10.1111/gwat.12024](https://doi.org/10.1111/gwat.12024)
- 764 Zs N, Kanli AI, Stickel J, Tillmann A (2010) The use of non-conventional  
765 CPTe data in determination of 3-D electrical resistivity distribution.  
766 *J Appl Geophys* 70(3):255–265. [https://doi.org/10.1016/j.jappgeo.](https://doi.org/10.1016/j.jappgeo.2010.01.008)  
767 [2010.01.008](https://doi.org/10.1016/j.jappgeo.2010.01.008)